JOURNAL OF AIRCRAFT
Vol. 43, No. 3, May–June 2006

Investigation of External Airbags for Rotorcraft Crashworthiness

Hyunsun Kim* and Bryn P. D. Kirby†
University of Bath, Bath, England BA2 7AY, United Kingdom

Airbags have commonly been implemented internally in automobiles for passenger safety, but they are considered for a variety of applications such as the landing system of the Mars Pathfinder to absorb the impact energy. This paper presents a feasibility study of an external airbag system for rotorcraft to improve the crashworthiness. It introduces a simple kinematic model for an external airbag system, which is validated against published experimental results of automobile airbags. Using a simplified helicopter geometry, several airbag system designs are investigated, and their potential benefits for crashworthiness are quantified. The results of this preliminary investigation show that an external airbag system is able to reduce fatalities, thereby significantly improving the crashworthiness of a rotorcraft.

Introduction

AN aircraft's crashworthiness is defined as the capability to protect the occupants from serious injury or death in cases of accidents that are potentially survivable.[1] This, therefore, has a direct implication on passenger safety. In the case of military aircraft, high recoverability of the airframe and onboard equipment also reduces the high associated costs.

Helicopters often fly at low speeds and low altitudes, and the associated energy upon impact is lower than that of fixed-wing aircraft. Improving the crashworthiness of helicopters has therefore been of much interest because of the potential for high survivability. One of the traditional methods for improving the crashworthiness has been to integrate energy-absorption mechanisms, such as a crushing subfloor structure and specifically designed landing gears and seats.[2] However, the increasing use of composite materials on helicopters brings further challenges for the crashworthiness design because of a lack of plastic deformation and the complicated failure modes of composite components.

Airbags have been implemented to improve the crashworthiness of automobiles since the 1970s. The common application is to install them internally where they are activated during a crash to protect the driver and passengers. Recently, an external installation of an airbag bumper system has been considered by automotive manufacturers.[3] Airbags are also being considered for a number of other applications, such as the landing systems of the Mars Pathfinder[4] and military airdrop platforms.[5]

A prototype of the external airbags for a helicopter crash protection system has recently been installed.‡ The system consists of several airbags, similar to those used in automobile applications, attached to the underside of the airframe. The airbags deploy just before impact to attenuate the impact energy. It was demonstrated from the crash tests that the system was able to limit fatalities and prevent damage to the airframe and the installed equipment. However, research in this field is limited, and to the authors' knowledge no specific numerical modeling of such a system for a helicopter has been published.

This paper presents a computational study of a rotorcraft external airbag system. A simple dynamic load model is developed based on Newton's law of motion, gas dynamics, and geometry of the system. The load model is then used for crash simulations using KRASH.[6] KRASH is kinematic crash analysis software that has been used in aircraft crash simulation for the past three decades. It employs a semi-empirical modeling approach using lumped masses and nonlinear springs to obtain the crash response of an airframe structure. Three airbag design configurations are tested numerically and compared against the crash response of the helicopter without airbags, in order to study the potential benefit of an airbag system.

Modeling Load Dynamics

An airbag is modeled as an ellipsoid attached to an impactor, as shown in Fig. 1. The impactor has mass m_I and impact velocity u_0. The airbag contains a volume of air V_B deployed at pressure P_B into a bag with negligible weight. The ellipsoidal airbag is defined by dimensions X and Y, Fig. 2. It is assumed that the airbag is fully deployed immediately before the impact such that it does not affect the aerodynamics of the impactor.

The impactor displacement s and velocity v_I can be represented by the differential equations (1)and (2).

$$\mathrm{d}s = u_0 \cdot \mathrm{d}t + \frac{1}{2}\frac{\mathrm{d}^2 s}{\mathrm{d}t^2}(\mathrm{d}t^2) \tag{1}$$

$$v_I = \frac{\mathrm{d}s}{\mathrm{d}t} = u_0 + \frac{\mathrm{d}^2 s}{\mathrm{d}t^2}\,\mathrm{d}t \tag{2}$$

From Newton's second law of motion,

$$\frac{\mathrm{d}^2 s}{\mathrm{d}t^2} = \frac{F}{m_I} \tag{3}$$

where F is the resultant force on the impactor, that is,

$$F = F_I - F_B \tag{4}$$

F_I is caused by the weight of the impactor, and F_B represents the force caused by the airbag pressure. Substituting Eq. (4) into Eq. (3) gives

$$\frac{\mathrm{d}^2 s}{\mathrm{d}t^2} = \frac{m_I g - (P_B - P_A)A_{\mathrm{eff}}}{m_I} \tag{5}$$

where g represents the gravitational acceleration, P_A is the atmospheric pressure, and A_{eff} is the effective area of contact between impactor and airbag. This can be obtained from the geometry of an ellipse

$$x^2/X^2 + y^2/Y^2 = 1 \tag{6}$$

Received 3 May 2005; accepted for publication 18 July 2005.

*Lecturer, Department of Mechanical Engineering; H.A.Kim@bath.ac.uk. Member AIAA.
†Student, Department of Mechanical Engineering.

‡Data available online at http://www.rafael.co.il/web/rafnew/products/air-reaps.htm [cited 24 Feb. 2004].

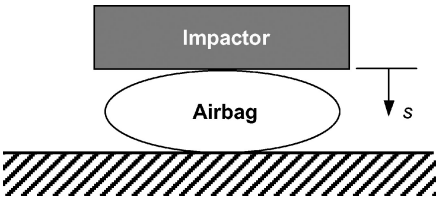

Fig. 1 Airbag and impactor model.

Fig. 2 Elliptical geometry of airbag.

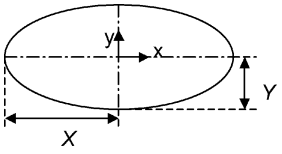

Assuming that the airbag geometry remains symmetrical about all three axes during crash, we can derive the expression for the circular effective contact area,

$$dA_{\text{eff}} = \pi X^2(1 - dy^2/Y^2) \tag{7}$$

and

$$dy = Y - ds/2 \tag{8}$$

Thus Eq. (7) becomes

$$dA_{\text{eff}} = (\pi X^2/Y)\, ds \tag{9}$$

The initial airbag volume V_{B0} is given by the volume of an ellipsoid

$$V_{B0} = (4\pi/3)X^2Y \tag{10}$$

Assuming a rigid airbag hence maintaining the profile of an ellipsoid during compression, the incremental change in volume is expressed as

$$dV_B = 2\pi x^2\, dy \tag{11}$$

Therefore, the change in airbag volume from the initial impact can be derived by integrating Eq. (11) from the initial position Y to the position y.

$$V_B = 2\pi X^2[(y - Y) - (y^3 - Y^3)/3Y^2] \tag{12}$$

The pressure inside the airbag is determined by assuming isentropic compression,

$$P_{B1}V_{B1}^{\gamma} = P_{B2}V_{B2}^{\gamma} \tag{13}$$

where $\gamma = 1.4$ for air and P_B and V_B are airbag pressure and volume, respectively, with subscripts 1 and 2 referring to the values at two arbitrary points in time.

Bag Stretching

To account for stretching of airbag fabric, we incorporate the bag stretch factor S, assuming a linear relationship between the airbag pressure and the increase in volume caused by stretching [Eq. (14)].

$$\frac{V_{B,\text{stretched}} - V_{B,\text{rigid}}}{V_{B,\text{rigid}}} = S(P_B - P_A) \tag{14}$$

Nieboer et al.[7] determined the empirical bag stretch factor $S = 2.0 \times 10^{-6}$ m^2/N from experimentation with automotive passenger bags; however, the material of the bag was not specified. For the comparative study, it was deemed reasonable to use the same bag stretch factor.

Bag Venting

Venting refers to escaping air from an airbag because of its permeability. It can also occur through airbag seams and specifically designed vents. Venting reduces the pressure inside the airbag and prevents the system from rebounding.

Assuming a constant rate of pressure reduction [Eq. (15)], Keshavaraj et al.[8] obtained the pressure rate constant k, again experimentally, for passenger bags. An average pressure leakage rate for ventless airbag systems, where venting can only occur through the fabric and seams, was found to be 205 kPa/s, whereas airbag systems with vents had a leakage rate of approximately 430 kPa/s.

$$\frac{dP}{dt} = k \tag{15}$$

This venting rate constant can be introduced to the isentropic pressure-volume relationship of Eq. (13) to give

$$P_B = P_{B0}\left(\frac{V_{B0}}{V_B}\right)^{\gamma} - \int k\, dt \tag{16}$$

Computational Implementation

For a given mass and initial velocity of the impactor and the geometry and the initial pressure of an airbag, the dynamic response of the airbag is obtained at discrete time steps. Based on the initial pressure of the airbag, the acceleration, hence the displacement and the force on the impactor, are computed using Eqs. (1–5). The change in the effective area of the airbag in contact with the impactor is computed from the displacement of the impactor [Eqs. (7) and (8)]. Bag stretching and venting are accounted for when updating the airbag pressure and volume [Eqs. (13), (14), and (16)].

This computation procedure is iterated over time until one of the following criteria is satisfied: the airbag volume is less than or equal to zero; the airbag pressure is less than atmospheric; or the impactor displacement becomes greater than the initial airbag height.

The procedure for dynamic modeling of an airbag (AIRBAGSIM) is outlined in Fig. 3.

Validation of the Load Dynamics Model

AIRBAGSIM dynamic model is validated against the experimental and finite element model results by Nieboer et al.,[7] which simulates passenger-bag interaction in automotive crash scenarios. Helicopter airbags differ from automotive passenger bags such that the impactor with a flat surface area is always greater than that of the airbag, and the effects of gravitational acceleration might not be ignored while the deployment is horizontal in an automotive crash scenario.

The experimental results for the 500-mm-diam impactor and the finite. element analysis results of 1000 mm diam are selected for validation, as they are of sufficiently large diameter for comparison. The experiment using a 500-mm-diam plate impactor had an impactor mass of 8.05 kg and an impact velocity of 4.70 m/s. The finite element model with a 1000-mm-diam plate impactor had a mass of 8.00 kg and an impact velocity of 24 m/s. Both tests were carried out on identical airbags of ellipsoid shape and with the geometry; $X = 296$ mm, $Y = 163.5$ mm. Sealed bags were used, that is, the venting pressure rate constant $k = 0$.

These two test cases are also simulated by AIRBAGSIM, and the results are plotted together with the experimental and finite element by Nieboer et al.[7] in Figs. 4 and 5. It can be seen that the AIRBAGSIM results are generally in good agreement with around 5% discrepancies.

Helicopter and Airbag Model Description

Kinematic Model of Helicopter

Kinematic crash analysis software KRASH is employed to investigate potential benefits of an external airbag system for an EH101 helicopter. The helicopter model used for analysis contains the basic airframe with two occupants (one pilot and one passenger) modeled by lumped masses and beam elements. Nonlinear spring elements

Do while $\{(V_B > 0)$ **AND** $(P_B \geq P_A)$ **AND** $(0 \leq s \leq \mathrm{Y})\}$,
Calculate acceleration, d^2s/dt^2 (5)
Calculate displacement, s (1)
Calculate impactor velocity, ds/dt (2)
Calculate resultant force, F (3)
Calculate y position (8)
Calculate effective area, A_{eff} (9)
Calculate airbag volume, V_B (12)
Calculate airbag pressure, P_B (13)

Account for bag stretching: starting from the airbag pressure and volume computed above, iterate to satisfy (13) and (14)

Account for bag venting: Calculate cumulative change in pressure due to venting, Σkdt, hence update airbag pressure, (16)

t = t + Δt
End do,

Fig. 3 AIRBAGSIM algorithm.

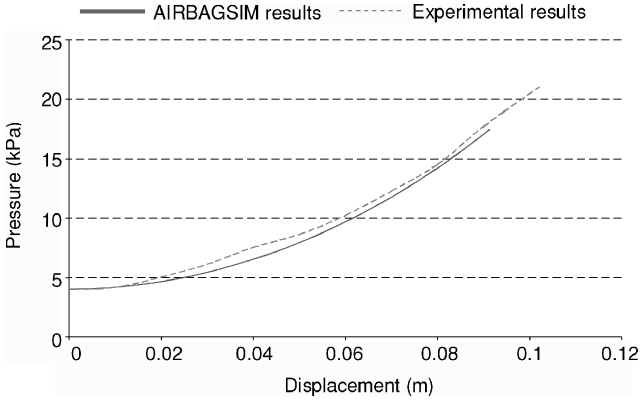

Fig. 4 Comparison with experimental results $m_I = 8.05$ kg, $u_0 = 4.70$ m/s, $P_{B0} = 4000$ Pa, $Y = 0.1635$ m, and $X = 0.296$ m.

with varying stiffness are attached to the underside the airframe to represent the stiffness of the belly panels. Two models used for the investigation are shown in Fig. 6, one with the undercarriage deployed and the other retracted.

A typical EH101 helicopter incorporates crashworthy "stroking" seats, which reduce the vertical acceleration experienced by its occupant. These are however replaced with nonstroking seats in the model, similar to those found on civil aircraft, in order to examine the effects of an external airbag system without the use of additional energy attenuating devices.

Design and Modelling of External Airbag System

The airbags are placed on the underside of the fuselage, an area of width 2.8 m and length around 9 m. The external airbag system considered in this investigation is comprised of two rows of seven airbags with each airbag having a diameter of 1.2 m. This two-row configuration gives a total width of 2.4 m and length of 8.4 m, covering most of the aircraft belly area.

Three airbag configurations are studied. The landing gear of EH101 provides the aircraft fuselage with a ground clearance of approximately 1 m; hence, this is chosen as the initial airbag height. This would mean that the landing gear and airbag system would come into contact with the ground simultaneously. The initial airbag volume is $754l$, which is in the region of 10 times the volume of a typical automotive airbag of 50–$100l$. Given that a typical gauge pressure of an automotive airbag is 34–48 kPa, the initial gauge pressure for a helicopter airbag is appropriately scaled down to 4 kPa. Airbags for this application would be designed with venting to avoid bouncing the aircraft on impact; hence, the rate of pressure drop due to venting k is set at 400 kPa/s. The impactor mass and velocity of 1000 kg and 10 m/s are specified, respectively. This configuration is henceforth referred to as airbag design 1.

Table 1 Number of springs per airbag

Mass point numbers	Total number of airbags	Number of springs per airbag
25–28	4	1
1–6 and 13–18	4	3
7–12 and 19–24	6	2

The second configuration, airbag design 2, is essentially identical to airbag design 1, with the exception of the airbag height. The airbag height is increased to 1.5 m giving a new initial volume of 1131 liters.

Airbag design 3 simulates airbags of airbag design 1 filled with air at atmospheric pressure, by setting a low initial airbag pressure of 10 Pa. To prevent rapid bag deflation, a reduced value of $k = 10$ kPa/s is specified.

In the KRASH model, there are 28 mass points representing the underside of the cockpit and cabin. If the airbag system is modeled by 14 mass points, each representing one airbag, it would generate extra load on the beams on the underside of the aircraft, because of the acceleration of the mass points without an airbag spring, as schematically represented in Fig. 7. It would be reasonable to assume that airbags produce uniformly distributed force over the area as they deform; hence, 14 airbags were modeled by attaching a spring to all 28 mass points, Fig. 8.

The number of springs used to represent each airbag is determined to be proportional to the density of mass points in that area of the base. Where there is more than one spring element per airbag, the airbag is modeled effectively by dividing into smaller airbags to produce the equivalent pressure. From Eqs. (3) and (5), it can be seen that the impactor mass and the effective contact area are directly proportional for constant pressure. However, the ellipsoidal geometrical constraint, Eq. (7) requires the effective area to be proportional to X^2 for a given height Y. The dimension of the smaller airbags is thus defined, depending on the number of spring elements. The number of spring elements per airbag is listed in Table 1. The length of the spring elements is the sum of the airbag height and the aircraft panel thickness.

Airbag Spring Properties

The stiffness of a spring element in KRASH is defined as three linear regions, as shown in Fig. 9. Airbag stiffness is nonlinear and

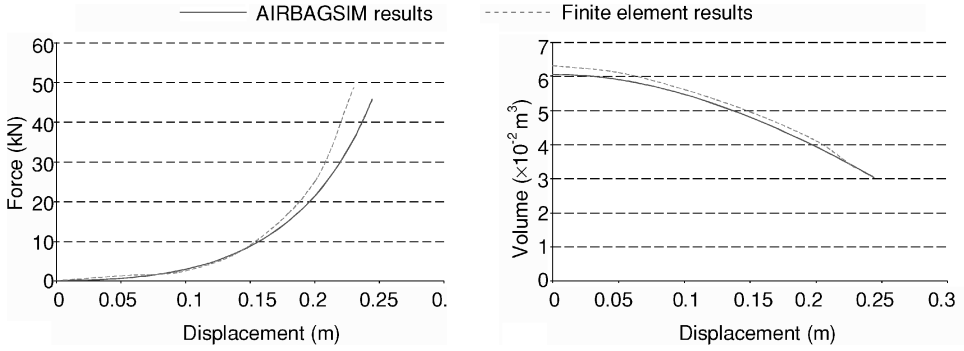

a) Airbag force vs impactor displacement b) Airbag volume vs impactor displacement

Fig. 5 Comparison with finite element results $m_I = 8$ kg, $u_0 = 25$ m/s, $P_{B0} = 4000$ Pa, $Y = 0.1635$ m, and $X = 0.296$ m.

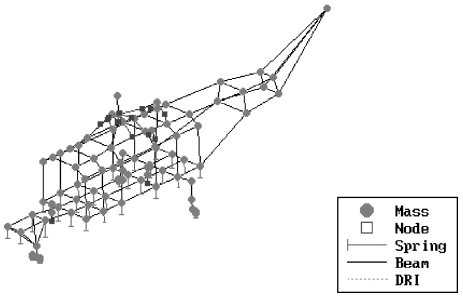

a) Undercarriage deployed

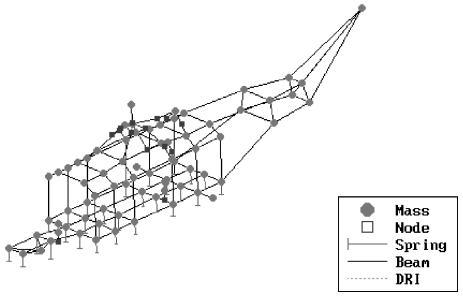

b) Undercarriage retracted

Fig. 6 EH101 KRASH models.

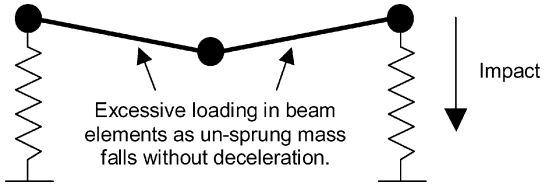

Fig. 7 Extra loading on beam elements caused by the mass point without an airbag spring.

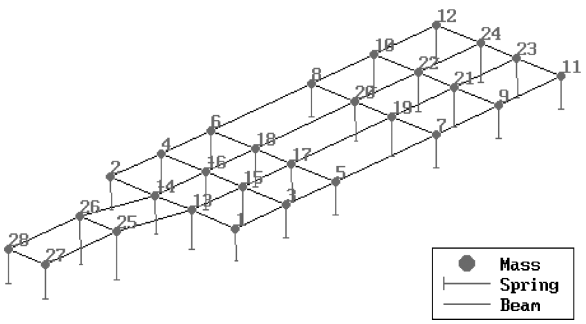

Fig. 8 KRASH model of airbag attachment.

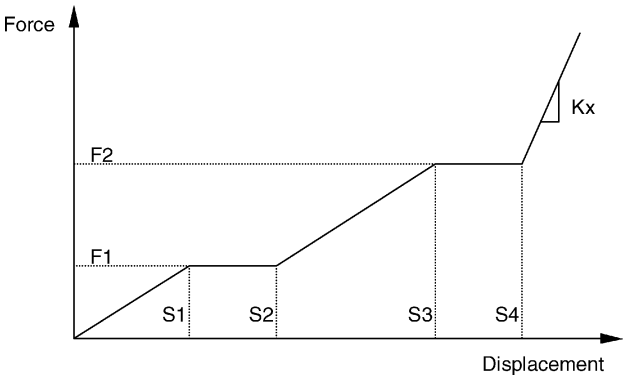

Fig. 9 Stiffness of KRASH spring element.

Table 2 Stiffness constants of airbag design 1 for KRASH

Mass points	25–28	7–12 and 19–24	1–6 and 13–18
S1, S2	0.47 m	0.47 m	0.47 m
S3, S4	0.72 m	0.72 m	0.72 m
F1	26.75 kN	13.37 kN	8.916 kN
F2	145.6 kN	72.83 kN	48.548 kN
Kx	1540 kN/m	770.2 kN/m	513.4 kN/m

Table 3 Stiffness constants of airbag design 2 for KRASH

Mass points	25–28	7–12 and 19–24	1–6 and 13–18
S1, S2	0.67 m	0.67 m	0.67 m
S3, S4	1.03 m	1.03 m	1.03 m
F1	17.58 kN	8.790 kN	5.860 kN
F2	103.6 kN	51.82 kN	34.54 kN
Kx	702.7 kN/m	351.3 kN/m	234.2 kN/m

Table 4 Stiffness constants of airbag design 3 for KRASH

Mass points	25–28	7–12 and 19–24	1–6 and 13–18
S1, S2	0.46 m	0.46 m	0.46 m
S3, S4	0.71 m	0.71 m	0.71 m
F1	31.11 kN	15.45 kN	10.30 kN
F2	144.6 kN	72.29 kN	48.19 kN
Kx	1378 kN/m	689.0 kN/m	459.3 kN/m

not in distinct linear regions, and therefore the stiffness constants are approximated.

To define the stiffness constants, the impact responses of airbag designs 1, 2, and 3 are analyzed using AIRBAGSIM. Figure 10 presents the impactor force variation against the displacement for airbag design 1. The nonlinear airbag stiffness is approximated, shown as the dotted line in Fig. 10, and the stiffness constants for airbag design 1 are listed in Table 2. Tables 3 and 4 summarize the spring stiffness constants for airbag designs 2 and 3, respectively.

Investigation of Crashworthiness

Description of Crash Scenarios

Defence Standard 00-970 sets the crashworthiness requirements of military aircraft for the United Kingdom Ministry of Defence.[9] It is primarily concerned with its capability to protect the occupants from serious injury or death in cases of accidents. In addition, it is desirable to ensure high survivability of the airframe and equipment to minimize the damage repair cost, particularly in the context of military aircraft.

For medium- to large-sized helicopters, the most severe crash case is a vertical collision onto a flat horizontal surface, which can lead to fatal spine injuries. To meet the most demanding level of crashworthiness requirements, an aircraft must survive a 95th percentile of potentially survivable crashes.[9] This requires the airframe to withstand a vertical impact of up to 13 m/s.

Three crash scenarios considered in this paper are listed in Table 5. It has been shown that forces exerted during severe helicopter crashes are often significantly greater than the static requirement; thus, the impact velocity of up to 15 m/s is applied.[10] Tests 1 and 2 with retracted undercarriage simulate landing-gear actuator failure, which is a more severe crash scenario than the requirement. Test 3 with the undercarriage deployed examines the interaction between the landing gear and an external airbag system. The main rotor lift of 1 *g* is specified for all tests.

Each of these crash scenarios is tested for all three airbag system designs described earlier and compared with the simulation results without an airbag system. The crashworthiness is examined by analyzing the acceleration of the mass points representing the pilot and a passenger in the cabin, which must not exceed the human tolerance level. The human tolerance level for acceleration vertically downwards is defined to be 25 g (Ref. 9). Another crashworthiness requirement considered in this investigation is the acceleration of the central engine located on top of the cabin, which must not fall into the cabin. These mass points are indicated in Fig. 11. The crash tests are simulated at 1×10^{-5} s time step.

Crash Simulation: Test 1

The vertical acceleration of the KRASH model without and with airbag designs 1, 2, and 3 for test 1 (11 m/s with undercarriage up) is shown in Fig. 12. Downwards acceleration is defined as negative, and zero time indicates the moment of impact. All three mass points experience an initial downwards acceleration, as expected. The oscillation of the accelerations can be interpreted to have two components: one with high amplitude and lower frequency representing the impact of the airframe with the ground, and the other with lower amplitude and higher frequency as a result of the localized structural response.

The benefit of external airbag systems can be clearly seen for all mass points, where the acceleration experienced is greatly reduced. The maximum acceleration is experienced later and over a longer period of time, in comparison with the results without airbags. The maximum vertical accelerations are summarized in Table 6. Airbag designs 1 and 3 are observed to offer a similar level of reduction in the peak accelerations, while airbag design 2 provides a superior performance because of its increased bag height. The acceleration of the pilot with airbag design 2 is found to be −21 g, which is almost 80% reduction from the no-airbag result and well within the safe limit of the human tolerance level.

Comparing the accelerations among the mass points reveals that the passenger experiences greater acceleration than the pilot. This is because of the elevated position of the pilot and the damping effects of the structure. This explains the further reduced level of the engine acceleration, which is located on top of the cabin. It can also be seen in all graphs of Fig. 12 that the secondary oscillation, which represents the structural response, is significantly reduced by the airbags. This indicates that less energy is attenuated by the structures, hence a reduced level of damage to the airframe.

Some high positive acceleration is observed beyond 0.15 s in Fig. 12. An analysis of energy in the system revealed that the kinetic energy starts to increase around this time. This represents an aircraft rebound because of the simplistic linear characterization of the airbag venting. However, in reality, the airbags would expel their contents during compression and bring the aircraft to a halt, and it is unlikely that the airbags would expand to bounce the aircraft back into the air. Moreover, deceleration following the initial impact would be of the greatest magnitude, and therefore the results beyond the point of rebound are ignored.

Crash Simulation: Test 2

Test 2 configuration is the same as test 1, but with a higher impact velocity of 15 m/s. The simulation results exhibit similar trends to those of test 1 but with higher magnitudes of acceleration, and are shown here for completeness in Fig. 13 and Table 7. The passenger experienced the greatest acceleration, followed by the pilot and the central engine. The reduction of up to 75% in the maximum acceleration is obtained in the case of the passenger with airbag design 2.

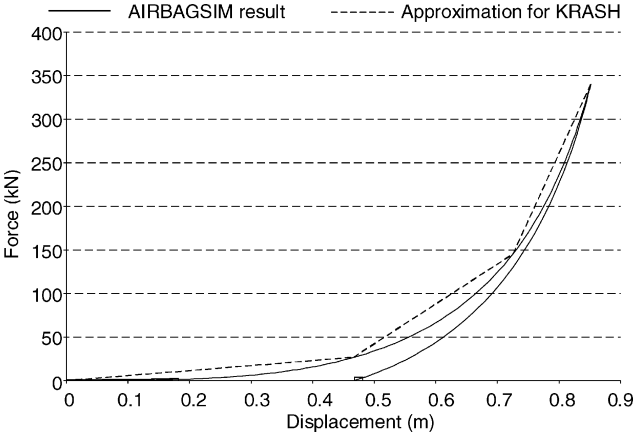

Fig. 10 Impactor force vs displacement for airbag design 1.

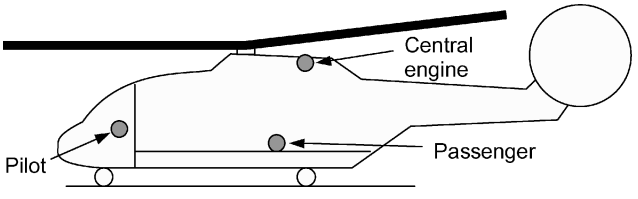

Fig. 11 Locations of mass points for pilot, passenger, and central engine.

Table 5 Crash scenarios

Test	Impact velocity, m/s	Undercarriage
1	11	Up
2	15	Up
3	15	Down

Table 6 Peak accelerations from test 1

Airbag design configuration	Pilot		Passenger		Central engine	
	Acceleration	%	Acceleration	%	Acceleration	%
Without airbags	−71 g	100	−140 g	100	−56 g	100
Airbag design 1	−36 g	51	−40 g	29	−37 g	66
Airbag design 2	−21 g	30	−30 g	21	−28 g	50
Airbag design 3	−33 g	46	−40 g	29	−37 g	66

Table 7 Peak accelerations from test 2

Airbag design configuration	Pilot		Passenger		Central engine	
	Acceleration	%	Acceleration	%	Acceleration	%
Without airbags	−160 g	100	−225 g	100	−58 g	100
Airbag design 1	−80 g	50	−77 g	34	−49 g	84
Airbag design 2	−60 g	38	−55 g	24	−39 g	67
Airbag design 3	−75 g	47	−70 g	31	−47 g	81

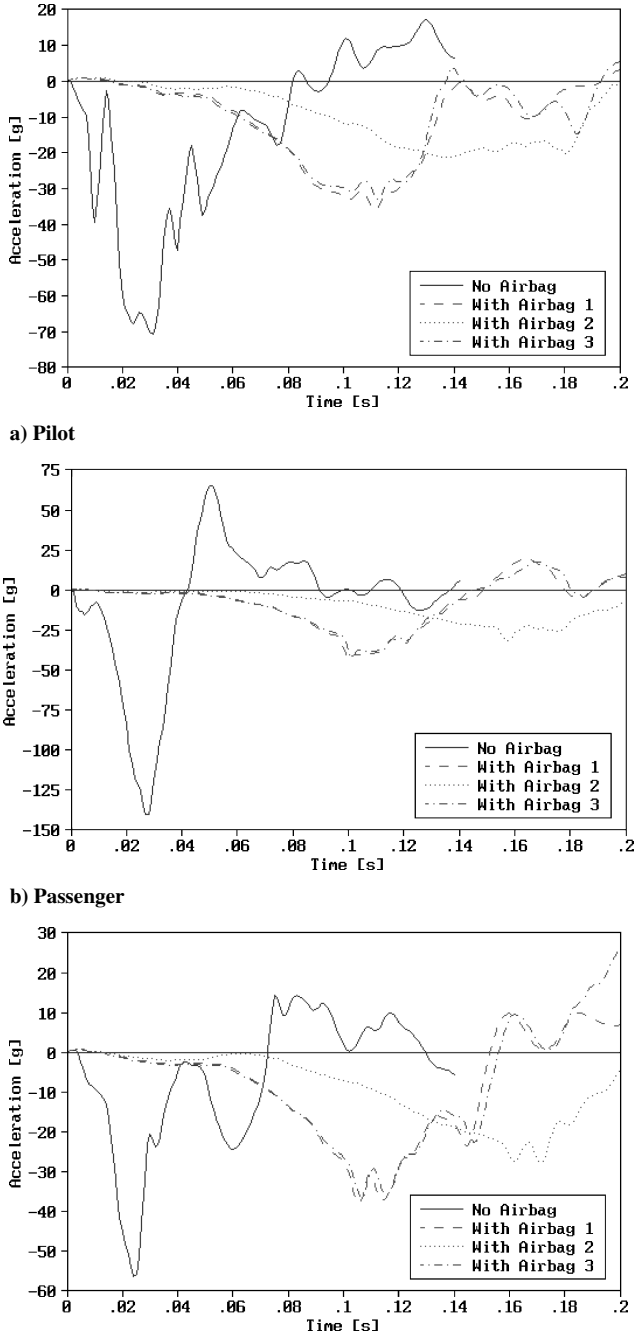

a) Pilot

b) Passenger

c) Central engine

Fig. 12 Vertical acceleration of test 1.

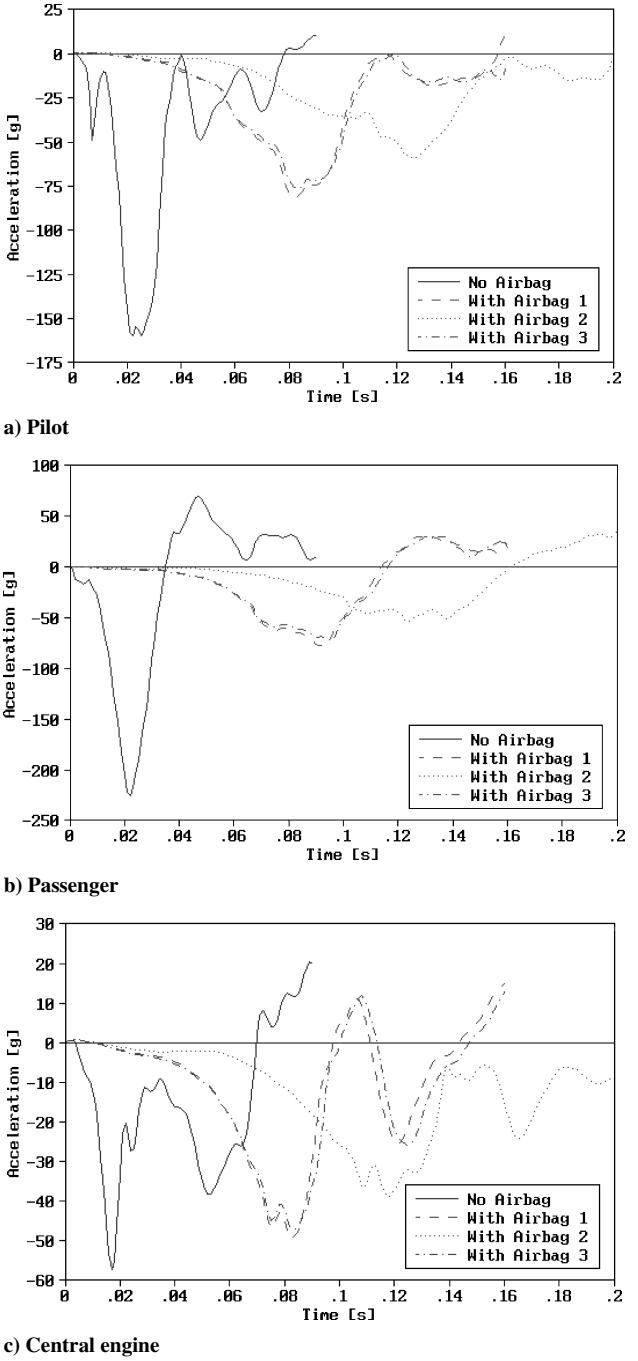

a) Pilot

b) Passenger

c) Central engine

Fig. 13 Vertical acceleration of test 2.

Airbag design 2 with the greater airbag height demonstrates the greatest benefit, although the acceleration experienced by all mass points considered for all tests is beyond the human tolerance level.

Crash Simulation: Test 3

Test 3 crash simulation has the same impact velocity as for test 2 but with a deployed undercarriage. The results are displayed in Fig. 14. The effects of the undercarriage can be clearly seen at the initial point of impact, where the response of the mass points, even for the case without airbags, is delayed by around 0.01 s as a result of the damping provided by the landing gears and tyres.

The behavior of the vertical accelerations in all cases is significantly different from tests 1 and 2, where the single peak immediately after impact is less prominent and the secondary oscillations are more dominant. The deceleration peaks are delayed for all configurations with and without airbag configurations. This indicates that

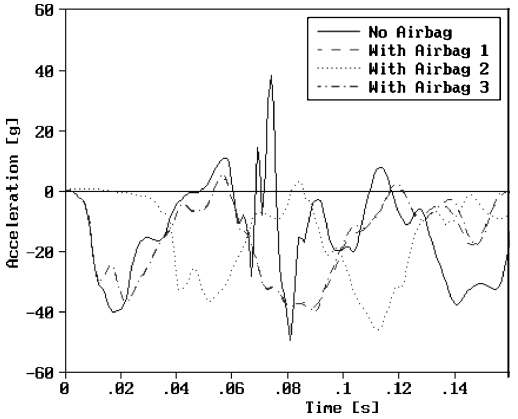

a) Pilot

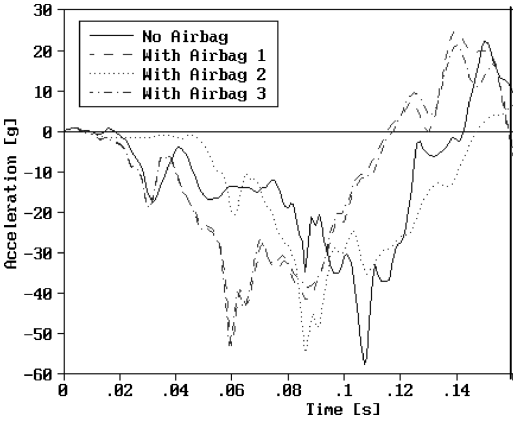

b) Passenger

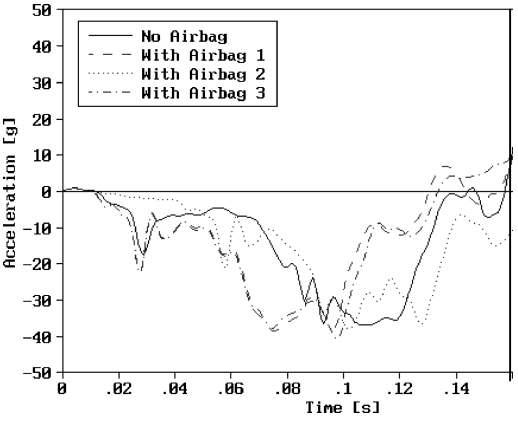

c) Central engine

Fig. 14 Vertical acceleration of test 3.

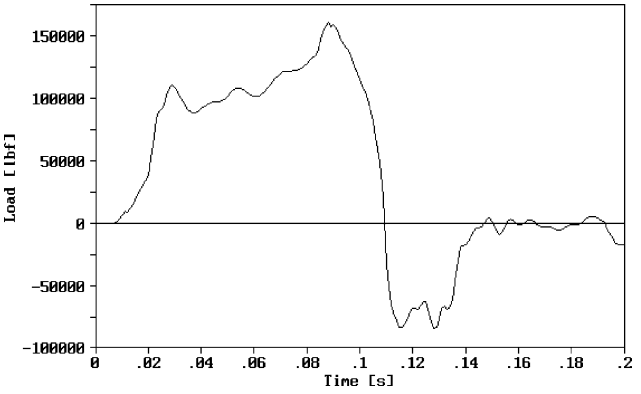

a) No airbags

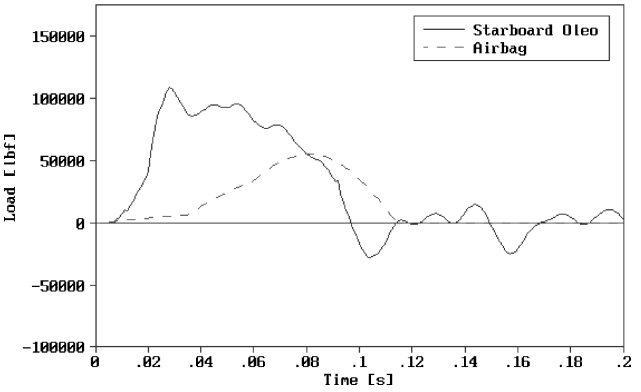

b) Airbag design 1

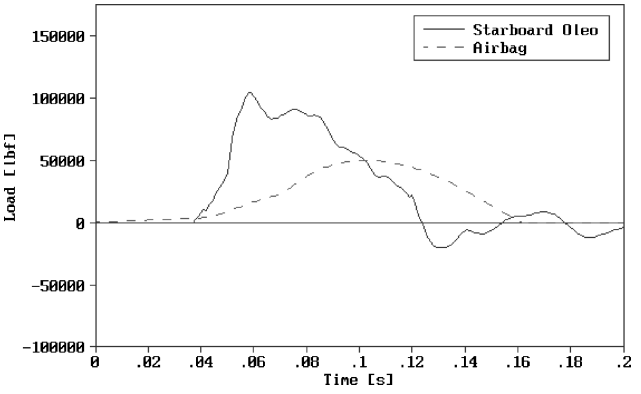

c) Airbag design 2

Fig. 15 Vertical load on oleo and airbag in test 3.

much of the energy is attenuated by the undercarriage. This is also evident in the mean acceleration levels, which are not significantly reduced by the installation of the airbags, unlike the previous tests.

It is observed that all three airbag systems give a similar acceleration profile, but the response of airbag design 2 is delayed by around 0.03 s compared with airbag designs 1 and 3 for all mass points. It can thus be deduced that an increased airbag height results in an acceleration lag but no significant effects in reducing the magnitude. This also indicates that the landing gear is dominant in attenuating energy for the crash scenarios studied.

The acceleration of the pilot Fig. 14a shows a sudden fluctuation of high magnitude between 0.07 and 0.08 s. However, it is unlikely that this high frequency and high-magnitude acceleration fluctuation would be experienced because of the inherent damping of the structure. Such behavior might be caused by the simplified lump-mass modeling approach employed here.

The interaction of the airbag systems and the undercarriage is further investigated by examining the vertical axial load transmitted through the oleo of the landing gear and through an airbag near the center of the cabin, Fig. 15. As the simulations with airbag designs 1 and 3 behave similarly, only airbag design 1 results are presented.

As shown in Fig. 15a, load on the oleo without airbags is transmitted from 0.007 s. This delay corresponds to initial compression of the tyre before oleo compression. The oleo compression reaches the maximum at 0.09 s. The variation in slopes up to the maximum is attributed to the oleo's damping properties and the interaction of the safety crash-release valves. After this peak, the level of load drops dramatically to a negative load, which represents the failure of the oleo element. This failure corresponds to the maximum aircraft acceleration, shown in Fig. 14. The load fluctuations around zero load from 0.15 s represent the structural vibration.

Figure 15b shows the interaction of an airbag in airbag design 1 with the undercarriage. It shows that the onset of load transmission through the airbag and oleo occurs at the same time because of their equal heights. The magnitude of load on the oleo rises rapidly up

to 0.03 s, as also seen in the simulation without airbags, Fig. 15a. However, it is from this point that the load on the oleo begins to reduce as the airbag load increases. Thus, the maximum oleo load experienced by the airbag configurations is less than that of the configuration without airbags. In addition, the sudden drop in the oleo load from the maximum at around 0.1 s is not observed in Fig. 15b, and the load on the oleo is reduced to zero at around 0.12 s, in comparison with around 0.15 s in Fig. 15a. Therefore, it is expected that the undercarriage would experience less damage.

The effects of the increased airbag height of airbag design 2 are displayed in Fig. 15c. In this configuration, load on the airbag starts to increase from the impact before the load on the oleo increases, as a result of the increased height. This leads to the delayed response observed in Fig. 14. The remaining load paths and the magnitudes however are similar to that of airbag design 1, as also observed in the acceleration response of Fig. 14.

Conclusions

This paper presents a simple modeling approach for airbag dynamics and helicopter crash response and investigates the potential benefit of external airbag systems. The crashworthiness requirements specified by the United Kingdom Ministry of Defence are used to examine the helicopter's crashworthiness, and the geometry of EH101 helicopter is employed for simulation in the kinematic crash analysis software, KRASH environment.

Three external airbag designs with varying bag height and pressure are studied. The airbag designs considered in this investigation are of a multiple airbag system covering the underside of the fuselage. Three vertical crash scenarios of varying impact velocities on flat ground with the undercarriage retracted and deployed for each airbag design are investigated and compared with the equivalent crashes without airbags. The maximum acceleration at the mass points representing the pilot, a passenger, and the central engine are selected to examine the crashworthiness. Although aircraft crashworthiness cannot be assessed on maximum acceleration alone, it is one of the primary concerns because of its influence on human survivability and is considered sufficient for the preliminary feasibility study.

With the retracted undercarriage configuration, the potential benefit of an external airbag system is significant. The maximum vertical acceleration decreases up to 79% in some cases, and a reduction in the oscillatory response of the structural dynamics can clearly be seen. The magnitudes of the maximum accelerations are still beyond the human tolerance level in most cases. However, the crash scenarios are more severe than the requirements, and an addition of crashworthy "stroking" seats incorporating energy-absorbing struts can reduce these values to an acceptable level. It is noted that although these seats are not modeled in the investigation presented they are already installed in many production helicopters.

The results from the crash scenarios and configurations considered in this study indicate that increasing the height of the airbags significantly improves the crashworthiness. However this needs to be considered in relation to the inflation system design. Airbag design 2 is almost 16,000 liters, 50% greater in volume than airbag design 1. The inflation would be rapid as an early deployment can have an unfavorable consequence on the aerodynamics of the helicopter, and the pyrotechnic system design may prove to be challenging.

However the effects of the initial airbag pressure are not found to be significant. In some cases, the airbags with the atmospheric pressure (airbag design 3) exhibit a slightly improved performance than that of the airbags with a high pressure (airbag design 1). This is because the atmospheric pressure, that is, lower pressure, exerts a lower force and decelerates the aircraft at a slower rate. Using the atmospheric pressure can be advantageous over a high pressure also in safety and the inflation system integration design.

The airbags show little improvement in crashworthiness of the helicopter when the undercarriage is deployed. It is observed that the landing gear is dominant in attenuating energy up to the initial peak of the load dynamics immediately after the impact. However, the airbags become more effective after the initial peak. It is evident that the airbags reduce the magnitude of the load experienced by the oleo, resulting in less damage to the undercarriage and possibly preventing a failure of the oleo. The benefit of the airbags might become more apparent if composite components are to be integrated in the landing-gear design.

The study presented in this paper demonstrates the potential benefit of an external airbag system in improving the crashworthiness of a rotorcraft. A further investigation using techniques such as finite element modeling would more accurately quantify the improvement. The United Kingdom Ministry of Defence guidelines[9] are used for the investigation. The U.S. military requirements are similar but with additional requirements for crashes with pitch and roll.[11] This can be achieved by adding airbags to the side of the fuselage. Crashes on water also need to be investigated, as many accidents occur over water.

Acknowledgment

The authors would like to thank Westland Helicopters, Ltd., for their advice and support for this project and for the permission to publish this work.

References

[1]"Aircraft Crash Environment and Human Tolerance," *Aircraft Crash Survival Design Guide*, ver. 2, Simula, Inc., USARTL-TR-79-22B, Phoenix, AZ, 1989.

[2]Prouty, R. W., *Military Helicopter Design Technology*, Jane's Information Group, Ltd., Surrey, England, United Kingdom, 1989, pp. 100–108.

[3]Clark, C. C., "The Crash Anticipating Extended Airbag Bumper Systems. National Highway Traffic Safety Administration," Society of Automotive Engineers, Ref. 946157, Washington, DC, May 1994.

[4]Cadogan, D., Sandy, C., and Grahne, M., "Development and Evaluation of the Mars Pathfinder Inflatable Airbag Landing System," *Acta Astronautica*, Vol. 50, No. 10, 2002, pp. 633–640.

[5]Patterson, T. F., "Design, Fabrication and Testing of an Airdrop Platform Utilizing Airbags as Shock Absorbers," Master's Thesis, Mechanical Engineering Dept., Northeastern Univ., Boston, June 1985.

[6]Gamon, M, and Wittlin, G., "DRI/KRASH KRWIN 2002 for Windows—User's Guide," Dynamic Response, Inc., CA, 2002.

[7]Nieboer, J. J., Wismans, J., and de Coo, P. J. A., "Airbag Modelling Techniques," *Society of Automotive Engineers Transactions*, Vol. 99, Sec. 6, 1990, pp. 1855–1870.

[8]Keshavaraj, R., Tock, R. W., and Nusholtz, G. S., "Simple Numerical Model (PRAM) for Simulation of the Passenger-Bag Interactions During Deployment of an Airbag," *Journal of Applied Polymer Science*, Vol. 67, No. 5, 1998, pp. 933–948.

[9]"Design and Airworthiness Requirements for Service Aircraft," Ministry of Defence, Defence Standard 00-970, Vol. 2, Book 1, Crown, Bristol, U.K., 1984.

[10]Richards, M., Smith, M., and Wittlin, G., "Airframe Water Impact Analysis Using a Combined MSC/DYTRAN—DRI/KRASH Approach," *Proceedings of the 1997 53rd Annual Forum of the American Helicopter Society Part 2*, American Helicopter Society, Alexandria, VA, May 1997.

[11]"Military Standard: Light Fixed and Rotary-Wing Aircraft Crash Resistance," U.S. Dept. of Defense, MIL-STD-1290A (AV), Washington, DC, Sept. 1988.